INVESTIGATIONS IN THE VACUUM ULTRAVIOLET USING A GRAZING INCIDENCE SPECTROGRAPH

LARRY EDWARD KAUFMAN

INVESTIGATIONS IN THE VACUUM ULTRAVIOLET

USING A GRAZING INCIDENCE SPECTROGRAPH

by

Larry Edward Kaufman
Lieutenant, United States Navy
B.S., Naval Academy, 1958

Submitted in partial fulfillment of the
requirements for the degree of

MASTER OF SCIENCE IN PHYSICS

from the

NAVAL POSTGRADUATE SCHOOL
June 1967

ABSTRACT

A grazing incidence vacuum spectrograph has been used for studies on high temperature plasmas and to investigate the Tungsten spectra produced by a vacuum spark source. The spectrograph uses a concave grating which has a 1-meter radius of curvature and 600 grooves per mm. Incident light strikes the grating at an angle of 8.15°, and the diffracted light is collected on a film strip (15-inches long, 35 mm SWR film) which is held along the Rowland circle.

Design and details of construction of the spectrograph and the vacuum spark source are presented. A total of 47 new Tungsten lines were identified from the vacuum spark source using Aluminum and Tungsten electrodes.

TABLE OF CONTENTS

Section		Page
1.	Introduction	9
2.	Vacuum Spark	9
3.	The Spectrograph	12
	3.1 Theory	12
	3.2 Mechanical Considerations	14
	3.3 Focusing	15
	3.4 Calibration	17
4.	Observations and Results	18
	4.1 Vacuum Spark Source	18
	4.2 Plasma Spectrum	23
5.	Conclusions and Recommendations	36
6.	Bibliography	55
	Appendix I	56
	Appendix II	57

LIST OF TABLES

Table		Page
I.	Identified Lines using Carbon and Aluminum Electrodes	19
II.	Spectrum of Tungsten and Aluminum using the Vacuum Spark Source	24
III.	Identified Lines of the Argon Plasma taken at the Midpoint of the Beam	37

LIST OF ILLUSTRATIONS

Figure		Page
1.	Portable Power Supply Console	41
2.	Assembly Drawing of the Trigger Spark-Gap Switch	42
3.	Ringing Frequency of Spark Gap	43
4.	Diagram of Vacuum Grating Spectrograph	44
5.	Blaze Angle Configurations	45
6.	Diagram of Grazing Incidence Spectrograph	46
7.	Top View of Spectrograph	47
8.	Side View of Spectrograph	48
9.	Photograph of Absorption Spectrum of Air	49
10.	Typical Results of Spark Gap Spectrum	50
11.	Spectrum of Carbon and Aluminum Electrodes	51
12.	Spectrum of Tungsten and Aluminum Electrodes	52
13.	Spectrum of Helium Plasma	53
14.	Spectrum of Argon Plasma	54

ACKNOWLEDGEMENTS

The continuing advice and assistance of Professor R. L. Kelly of the Naval Postgraduate School is gratefully acknowledged.

I also express my appreciation to Messieurs R. C. Moeller and R. A. Garcia for their technical support.

1. Introduction

A steady-state plasma system is in operation at the Plasma Laboratory at the Naval Postgraduate School. Numerous probe measurement experiments have previously been conducted on the plasma system to determine the electron density and temperature. It was desirable to identify the impurities associated with the system and to determine the ionization states of the ionized atom. Since the most intense lines for three-and four-times ionized atoms occur in the vacuum ultraviolet region, the use for a grazing incidence spectrograph is necessary for their observation. A survey spectrograph had been built by R. L. Kelly, but focusing had not been completed. A vacuum spark light source was designed and built for use in focusing the spectrograph.

This report describes the design, construction, and operating parameters of the vacuum spark light source; the focusing, calibration, and optical considerations of the spectrograph; the identification of the impurities associated with the plasma system; and the identification of the spectra of Carbon, Aluminum, and Tungsten obtained from the vacuum spark source.

2. Vacuum Spark Source

In this light source a gap of a few millimeters separates a pair of electrodes, which are held in a vacuum and which are connected to a capacitor charged to some tens of kilovolts. Breakdown is controlled by a spark-gap switch in the power supply console. The power supply (consisting of a thyratron circuit, a trigger circuit, and a charging circuit) is housed in a portable console, as shown in Figure 1. The thyratron circuit has a

variable output of up to 10 kilovolts. A 5C22 hydrogen-filled thyratron is held at ground potential until a trigger pulse fires the thyratron. The trigger circuit employs a standard EFP pentode with a variable input of 2 kilovolts; an output pulse with a rise time of less than 8 ηs and pulse width of 2×10^{-7} seconds is generated by this circuit. The charging circuit consists of a low inductance, high voltage capacitor of 0.5 μf connected to a 20 kilovolt variable power supply.

The spark-gap switch is basically the same type as reported by Lupton [1]. Figure 2 is an assembly drawing of the switch. The cathode and anode are made of cylindrical brass stock with the ends rounded to form hemispheres of 1¼ inch diameter. The trigger pin (which is connected to the thyratron circuit) is brought through the cathode in a teflon insulator. The backstrap is spaced very closely to the electrodes, but is insulated from the anode by a Mylar sheet. The function of this arrangement is to reduce erosion of the narrow arcing points where the holdoff voltage is established; the magnetic force caused by the load current flowing through the connecting backstrap during discharge repels the electric arc to the outward surface of the switch electrodes.

The spark-gap switch is mounted on top of the capacitor. The spacing between the brass electrodes of the spark-gap switch is set to determine the breakdown voltage. This gap setting can easily be varied to hold off any voltage up to the maximum input voltage of 20 kilovolts. For example, a spacing of 6 mm is sufficient to hold off 18 kilovolts.

After the spark-gap switch has been set to hold off the desired voltage, the trigger circuit is actuated either by using a manual push button located on the front of the power supply, or by using a timer with a 15 second on/off cam. The activation of the trigger circuit permits the thyratron circuit to deliver a 10 kilovolt pulse to the trigger pin of the spark-gap switch as shown in Figure 2. This pulse ionizes the gas between the brass electrodes, reducing the effective gap of the electrodes sufficiently for the switch to fire.

The spark-gap switch in the power supply console is connected electrically across a glass pipe T which is attached to the front of the spectrograph. The end plates for the glass T hold the electrodes, one of which is fixed and the other adjustable. The electrodes are under the same vacuum as the spectrograph so their gap setting must be made considerably less than that for the spark-gap switch if the switch is to control the spark. For instance, at a pressure of 2 microns, the gap setting of the electrodes is only 2 mm with the spark-gap switch set for a breakdown voltage of 18 kilovolts. The voltage breakdown of the spark-gap switch provides the path for the voltage to appear across the glass electrode holder. The glass T electrode holder is shown with the portable power supply console in Figure 1.

An extremely low inductance is mandatory where high values of peak current are desired. The inductance of the circuit at a breakdown voltage of 15 kilovolts was found to be 1.20 micro-henrys, giving a ringing frequency of 206 kilocycles. The ringing frequency is shown in Figure 3. The inductance of the

0.5 μf capacitor used in the charging circuit was 0.025 microhenrys. The circuit inductance is higher than anticipated, and may have to be reduced to obtain larger spark currents.

3. Spectrograph

3.1 Theory

The theory of the concave grating has been discussed in detail by Beutler [2], by Mack, Stehn, and Edlen [3], with recent contributions by Namioka [4]. Only the basic Rowland conditions will be presented in this report.

If a concave grating of radius ρ is tangent to a circle of diameter ρ, the spectrum will be focused in the circle if the entrance slit is also in the circle. More precisely, if φ is the angle at the grating between the normal to the grating and the incident light, with ψ the angle of diffraction, then:

$$\frac{ds}{d\lambda} = \frac{\rho}{e \cdot \cos\psi} \tag{1}$$

where s is the distance along the Rowland circle form the central image to the position of a spectral line of wavelength λ, and e is the distance between the grooves of the grating. Figure 4 shows a diagram of a vacuum grating spectrograph at grazing incidence.

For $\frac{1}{e}$ =600 grooves/mm and ρ=1 meter:

ψ	$d\lambda/ds$
0°	16.7 A/mm
70	5.71
75	4.32
80	2.90
81.5	2.48
82	1.45

Upon integrating equation (1) we obtain:

$$\lambda = e(\sin\varphi - \sin\psi) \tag{2}$$

The distance from the center of the grating to a point on the Rowland circle is given by 2R cos ψ, as shown in Figure 4.

Gratings are usually "blazed" in such a way as to throw most of the diffracted energy into a particular region of the spectrum. It has been shown by Wood [5] that as much as 75% of the incident light can be directed into a particular order with a sharp blaze. Figure 5 shows the two ways in which the blaze angle can be used. The equation relating blaze wavelength to the angle of incidence is:

$$\pm \lambda_B = \frac{e}{m} \sin(\varphi \pm 2\alpha) - \frac{e}{m} \sin \varphi \tag{3}$$

where m is the order of diffraction, φ the angle of incidence, and α the blaze angle. The plus and minus signs result from the fact that the incident light may be brought to the grating at an angle on either side of the normal, as seen in Figure 5. The result is that the blaze direction is either $\varphi+2\alpha$ or $\varphi-2\alpha$. With a blaze angle of 4° 45':

φ	$+\lambda_B(m=1)$	$-\lambda_B(m=1)$
0°	2760 A	2760 A
10	2650	2755
20	2505	2672
30	2271	2505
40	1954	2255
50	1587	1954
60	1186	1570
70	723	1164
80	251	701
81.5	184	634

Only the arrangement utilizing $\varphi-2\alpha$ is useful at grazing incidence.

The grating used in this research was a Bausch and Lomb replica, type 472, with a one meter radius of curvature and 600 grooves per mm. The blaze angle of the grating was 4° 45', with a blaze wavelength of 634A at an angle of incidence of 81.5°.

3.2 Mechanical Considerations

The decrease in reflection at normal incidence of all grating material necessitates the use of grazing incidence spectrographs for wavelength below 1000A. At normal incidence, the best reflection for the range 1000A to 500A is shown by platinum, which has about 24 percent reflectance at 584A [6]. Below 500A, reflectances at small angles are very poor, with a 1-3 percent reflectance for platinum at 303A [7]. At grazing incidence, most metals show good reflectivity. However, there is a short wavelength cut-off which depends on the angle of incidence, the light source, the detector, and other factors. The Naval Postgraduate School spectrograph is designed so that an angle of incidence of approximately 82° will cover the wavelength region from about 150A to 2250A on a 15 inch strip of film. Mechanical considerations set the angle of incidence at 81.5°.

The basic features of the spectrograph are shown in Figure 6. It is made of non-magnetic materials because of its use in rather large magnetic fields. The slit assembly is held in a tube which is welded into the front plate. The grating and film holder are supported by a channel beam which is bolted to the front plate, as shown in Figure 7.

The film holder consists of four plates of Aluminum which have been shaped on one edge to a diameter of one meter. The

plates are bolted together in pairs and spaced to accept 35 mm film.

The slit assembly consists of three plates housed in a two-inch diameter brass tube. The front plate has a rectangular opening covered by stellite slit jaws that form the entrance slit. The second plate eliminates light which might reflect directly off the walls of the tube onto the film. The third plate consists of adjustable brass plates which control the aperture of the grating. The Rowland circle conditions and the positions of the slit, grating, and film holder can best be seen in Figures 6 and 7.

The vacuum envelope consists of a 10-inch Aluminum tube which bolts to the front plate and which has a back plate bolted onto it. To allow film loading in daylight, a changing bag is fastened around the back plate. The back plate is removed inside the changing bag, the film is slid into the channel of the film holder, and the back plate is bolted on. The exposure time is controlled by a gate valve which also serves to isolate the spectrograph from the system being tested. The gate valve and the connection to the plasma system are shown in Figure 8.

3.3 Focusing

The adjustment and focusing of the grazing incidence spectrograph are dependent upon the accurate positioning of the slit, grating, and film holder. With increasing angle of incidence, the astigmatism of the grating increases rapidly. Further, it becomes very important that the slit be parallel to the grooves

of the grating to achieve good resolving power. The resolving power of a grating will increase as the slit width is decreased. However, it has been shown by Mack, Stehn, and Edlen [6], that the resolving power below about 200A is limited not by the grating, but rather by the finite slit width that must be used to avoid clogging of the slit by the particles from a spark source. Slit widths are therefore usually not less than about 4 microns. In order to obtain sufficient intensities, the entrance slit of the Naval Postgraduate School spectrograph was set at 15 microns for all survey work up to the present. Thus, the resolving power of this spectrograph is not as high as can be achieved.

To help in the positioning of the equipment, a template was used that matched the radius of the Rowland circle. Templates can be made from either wood or cardboard, and both types were used in the focusing runs. Since the distances are known between the slit, grating, and the central image, the template can be used to fix the rough position of the trio. Whenever readjustments were necessary, the template was used to reposition the grating; since the slit mounting and film holder are non-adjustable after their initial positions are fixed, the grating provides the sole adjustment to the system.

As much of the focusing as possible was done in air, with two methods being used. The Rowland circle can be extended, as shown in Figure 6, until the visible spectrum can be seen. The spectrograph can then be focused for two points on the circle, such as the central image and the visible Hg 5461A line. All the other wavelengths will then be in focus to a first approxi-

mation. The second method utilizes the short wavelength continuous spectrum of the mercury lamp to obtain the absorption spectrum of air. Sharp absorption lines indicate good focus at the long wavelength end of the spectrograph. If the film fits the focal curve of the camera holder correctly, this procedure also brings all shorter wavelengths into focus. An example of the absorption spectrum taken with the spectrograph is shown in Figure 9.

The preliminary adjustments can be done in air, but the final adjustments must be done in a vacuum. All of the focusing runs were done at a pressure of 2-3 microns, using the vacuum spark with Carbon and Aluminum electrodes. The Aluminum spectrum adequately covers the entire region between 150A and 2250A, and Carbon gives lines that are easy to identify. Focus runs using 200 sparks at 18 kilovolts gave spectra of good intensity. A total of 30 runs was necessary to focus the spectrograph. Figure 10 shows the resolving power achieved when the spectrograph was in good adjustment.

3.4 Calibration

Many of the calibration calculations were done with the aid of the computer. A computer program was written from the grating equation, with the print-out including distances from an arbitrary reference point and the dispersion at given wavelengths. The program is given in Appendix I. The position of lines were calculated relative to C IV λ 1548, C III λ 977, and C IV λ 384 becuase of their prominence. The obvious Carbon and Oxygen lines were identified initially, with the computer

program then being interpolated to position the remaining lines. The wavelengths and intensities were then compared with those found in the book by Kelly [8].

In later work, a program using least square curve fitting with orthogonal polynomials was used [9]. This program is discussed in Appendix II. To use this program, the film strip must be measured accurately with regard to position. The lines with known wavelength and position are used for the original abscissas, and the unknown line positions form the data card deck. The program computes the wavelength associated with the unknown line position and also computes the error of the original abscissa points. When the position points are limited to cover only about 400A of the spectrum, the program is capable of computing wavelengths within ± 0.2 A of the actual value with a few iterations. For greater accuracy, it is necessary to increase the number of original abscissa points, and to disregard all broad lines. It must be emphasized that either program can only be as accurate as the line positions, and erroneous line positions when recognized must be omitted.

4. Observations and Results

4.1 Vacuum Spark Source

Runs using Carbon and Aluminum were conducted at a breakdown voltage of 18 kilovolts with the spectrograph at a pressure of 2 microns. The exposure time was determined by the time necessary to apply 200 sparks to the system. Figure 11 shows an exposure made with the vacuum spark source using Carbon

TABLE I

IDENTIFIED LINES USING CARBON AND ALUMINUM ELECTRODES

λ	IDENTIFICATION
215.128	OV
220.352	OIV
238.467	Al VI
243.760	Al VI
259.506	C IV
278.699	Al V
281.397	Al V
303.740	O III
307.248	Al VI
308.560	Al VI
309.012	Al VII
309.596	Al VI
310,908	Al VI
312.241	Al VI
320.146	Al IV (2x160.073)
320.979	O III
323.372	Al IV (2x161.686)
384.032	C III
384.178	C III
419.620	C IV
459.462	C III
459.521	C III
476.934	Al VI (2x238.467)
480.219	Al IV (3x160.073)
485.058	Al IV (3x161.686)
487.520	Al IV (2x243.760)
499.462	C III
499.530	C III
507.391	O III
507.683	O III
508.182	O III
519.012	C IV (2x259.506)
525.795	O III
538.256	O II
538.433	O II
599.598	O III
607.480	O III (2x303.740)
614.496	Al VI (2x307.248)
617.120	Al VI (2x308.560)
618.024	Al VII (2x309.012)

TABLE I continued

λ	IDENTIFICATION
619.192	Al VI (2x309.596)
621.816	Al VI (2x310.908)
624.482	Al VI (2x312.241)
629.732	O V
640.292	Al VI (4x160.073)
646.744	Al VI (4x161.686)
702.322	O III
702.822	O III
702.899	O III
703.850	O III
715.401	Al VI (3x238.467)
718.484	O II
718.562	O II
731.280	Al VI (3x243.760)
778.518	C IV (3x259.506)
787.710	O IV
790.103	O IV
790.203	O IV
832.754	O II
832.927	O III
833.326	O II
833.742	O III
834.462	O II
835.096	O III
835.292	O III
858.094	C II
858.561	C II
903.950	C II
904.134	C II
911.220	O III (3x303.740)
921.744	Al VI (3x307.248)
925.680	Al VI (3x308.560)
927.036	Al VII (3x309.012)
928.788	Al VI (3x309.596)
932.724	Al VI (3x310.908)
936.723	Al VI (3x312.241)
977.026	C III
1009.854	C II
1010.074	C II
1010.369	C II

TABLE I concluded

λ	IDENTIFICATION
1036.330	C II
1037.020	C II
1076.512	O II (2x538.256)
1076.866	O II (2x538.433)
1174.916	C III
1175.700	C III
1176.351	C III
1214.960	O III (4x303.740)
1247.368	C III
1323.916	C II
1334.520	C II
1335.692	C II
1548.195	C II
1550.768	C IV
1560.687	C I
1605.776	Al III
1611.849	Al III
1670.810	Al II
1719.430	Al II
1712.279	Al II
1724.981	Al II
1760.103	Al II
1761.979	Al II
1763.892	Al I
1763.947	Al II
1765.811	Al II
1767.735	Al II
1854.720	Al III
1855.928	Al II
1858.031	Al II
1859.990	Al II
1862.318	Al II
1862.795	Al III
1930.902	C I
1930.930	C I
1931.927	C III
1990.530	Al II

and Aluminum electrodes. The lines are identified in Table I. Good resolution of the O II and O III groups at 834A was indicated. Al VII was the highest ionization state obtained.

The vacuum spark was utilized to investigate the Tungsten spectrum. Since it was felt that the previous work in Aluminum would provide good calibration points for the Tungsten spectrum, the spark source was used with Aluminum and Tungsten electrodes. Runs were conducted under the same conditions as previously stated. Figure 12 shows an exposure of the spectrum obtained with the lines identified in Table II. Most of the lines of this spectrum were not found in the literature [8]. The least-square-curve-fitting computer program was used for this spectrum with a total of 150 abscissa points (known lines of C, Al, O, and N), and 106 unknowns. The average error between the original and computed abscissa values was found to be ± 0.05A. It was reasonable to assume that the unidentified lines in the spectrum should also be accurate to within ± 0.05A.

The last column in Table II lists the elements that have a known line within ± 0.3A of the unidentified wavelength shown. Those unidentified lines with no element listed except Tungsten are assumed to be Tungsten lines. Several elements which have been studied extensively, and which have many lines, have nevertheless been excluded from consideration. These include Bi, Cu, Cl, F, Hg, Pd, Sc, and Zn.

The shortest wavelength identified in using the spark source was in the O IV group at 150A. Some lines did appear at shorter wavelengths, but they were so faint that accurate identification

was impossible. It appears that the short wavelength end of the spectrum is limited by the grating (a platinum-coated grating has recently been obtained to improve intensities at short wavelengths).

4.2 Plasma Spectrum

The plasma system at the Naval Postgraduate School consists of a nine-foot long assembly of four-inch pyrex sections with access ports at 14-inch intervals. The continuous plasma source is a hollow cathode discharge operating in a reflex configuration at a cathode pressure of one micron. The longitudinal magnetic field is variable up to 10,000 gauss, and the discharge carries up to 200 amps at 140 volts.

The sprectrograph was used to investigate the elements and stages of ionization in this plasma system. The spectrograph was set up to look across the line of plasma at a position midpoint down the stream. Exposure times of up to seven minutes were necessary with the discharge at 100 amps and 140 volts. Various magnetic fields were used, with the majority of runs being made at 1000 gauss.

Figure 13 shows an exposure of the Helium plasma obtained from the system. These lines were used to calibrate the spectrograph for use with an Argon plasma. Figure 14 shows the spectrum from the Argon plasma. The lines are identified in Table III.

The observation of O IV in the Argon plasma shows that there are electrons with energies of at least 77 volts, while the absence of O V shows there cannot be many with energies as high as 114 volts. The argon plasma also showed very few lines at the long wavelength end of the spectrum. This may be due to the blaze angle of the grating being used.

TABLE II

SPECTRUM OF TUNGSTEN AND ALUMINUM USING THE SPARK GAP SOURCE

λ	INT*	IDENTIFICATION
150.088	30	O VI
150.124	30	O VI
160.073	30	Al IV
161.686	30	Al IV
172.168	30	O V
172.935	10	O VI
173.082	10	O VI
192.751	50	O V
192.800	50	O V
192.906	50	O V
194.593	30	O V
197.007	10	N IV
198.031	30	O V
198.7	30	W ? Mo VII ?
199.2	30	W ?
199.6	30	W ? Ti VII ?
200.3	30	W ?
201.8	10	W ? Ti VI ?
202.191	10	O V
202.226	10	O V
202.282	10	O V
203.836	70	O V
207.183	70	O IV
207.229	70	O IV
207.794	70	O V
214.032	50	O IV
215.245	50	O V
216.018	100	O V
216.3	70	W ? Ni VII ?
220.352	100	O V
221.1	10	W ?
221.648	30	O IV
222.791	50	C IV
223.9	70	W ? Fe VIII ? Co III ?
225.299	30	O IV
226.2	30	W ? Ni VII ? Co VII ?
227.468	70	O V
227.549	70	O V
231.101	100	O IV
231.200	100	O IV

TABLE II continued

λ	INT	IDENTIFICATION
231.823	50	O V
233.561	100	O IV
233.596	100	O IV
238.361	100	O IV
238.573	100	O IV
239.030	70	Al VII
240.770	50	Al VII
242.140	10	O IV
243.760	100	Al VI
246.563	10	O IV
247.563	10	N V
248.5	50	W
249.7	30	W ? Mn VII ?
250.2	50	W
251.347	50	Al VIII
252.3	30	W
252.564	30	O IV
253.082	30	O IV
253.8	30	W ?
254.3	50	W ?
254.6	50	W ?
255.5	30	W ? Mo VII ?
256.0	10	W ?
259.0	30	W
259.127	30	Al VII
259.458	30	Al IV (2x129.729)
260.389	70	O IV
260.556	70	O IV
261.219	70	Al VII
261.696	70	Al V (2x130.848)
263.768	10	O III
265.260	10	Al V (2x132.630)
266.932	50	O IV
268.0	30	W ?
268.6	30	W ?
268.9	30	W
269.9	50	W
270.583	50	C III
272.270	100	O III
274.6	50	W

TABLE II continued

λ	INT	IDENTIFICATION
275.366	70	O III
276.108	30	O V
276.5	70	W ? Co VI ?
278.699	100	Al V
279.1	50	W ? Co VI ?
279.456	50	O IV
279.633	50	O IV
279.937	70	O IV
281.397	100	Al V
283.420	50	N IV
284.042	50	Al IX
285.467	70	Al VIII
285.714	70	O IV
285.838	70	O IV
286.448	30	O V
289.230	50	C IV
295.657	30	O III
300.176	50	O VI (2x150.088)
300.248	50	O VI (2x150.124)
303.799	30	O III
305.596	70	O III
305.703	70	O III
305.836	70	O III
307.248	70	Al VI
308.560	70	Al VI
309.012	70	Al VII
309.596	100	Al VI
309.852	100	Al VI
310.908	70	Al VI
312.418	70	C IV
312.455	70	C IV
320.146	50	Al IV (2x160.073)
320.979	70	O III
323.372	70	Al IV (2x161.686)
324.8	50	W ?
325.4	30	W
328.200	50	Al VIII
328.742	50	O III
329.4	50	W ? Mn VI ?
332.891	50	Al X
333.8	30	W ?

TABLE II continued

λ	INT	IDENTIFICATION	
334.3	30	W	
336.0	50	W ?	
338.7	30	W ?	
343.290	50	Al	VII
343.650	50	Al	VII
344.336	50	O	V (2x172.168)
345.309	30	O	III
345.870	70	O	VI(2x173.082)
349.116	50	O	V (2x174.558)
351.1	50	W ?	Mg V ?
352.160	70	Al	VII
353.000	70	C	III
353.9	70	W	
354.2	50	W ?	Mg V ?
355.137	50	O	III
355.333	50	O	III
356.900	70	W	
359.016	30	O	III
359.223	30	O	III
367.7	50	W ?	Mg VII ?
368.0	50	W ?	Mg IX ?
371.2	50	W ?	
373.805	100	O	III
376.1	30	W ?	
376.3	30	W ?	
377.8	30	W ?	Mo VI ?
379.505	30	O	III
380.7	10	W ?	Ti VI ?
381.689	70	Al	VIII
384.105	70	C	IV
385.0	70	W ?	Ti V ?
385.505	70	O	V (2x192.751)
387.398	50	O	III
387.639	50	O	III
388.8	50	W ?	Ti V ? C II ?
389.187	30	Al	V (3x129.729)
390.8	30	W ?	
391.943	30	O	II
392.544	30	Al	V (3x130.848)
393.8	100	W ?	

TABLE II continued

λ	INT	IDENTIFICATION
395.0	50	W
396.062	40	O V (2x198.031)
397.120	50	O III
398.4	30	W ? (2x199.2)
399.2	30	W ? Ti VII ? (2x199.6)
400.2	40	W ?
400.6	40	W ? (2x200.3)
401.182	30	Al X
401.7	30	W ? Mn V ? Fe V ?
403.035	40	O II
403.300	40	O II
403.9	50	W ? Mn V ?
404.3	50	W
407.3	100	W
408.5	30	W ? Mn V ?
410.0	30	W ? Mn V ?
410.5	30	W ? Mo V ? Fe V ?
410.9	30	W
414.0	50	W ?
415.0	70	W
415.588	50	O V (2x207.794)
418.0	30	W ? Fe V ?
419.620	50	C IV
421.6	30	W
422.1	30	W ? Mn V ? Fe V ?
428.064	50	O IV (2x214.032)
430.041	70	O II
430.177	70	O II
431.6	50	W ? Mo V ? Fe V ?
432.036	50	O V (2x216.018)
434.646	30	O III
438.5	30	W
440.5	70	W
444.6	30	W ?
445.638	30	O II
447.5	50	W
450.264	70	O VI (3x150.088)
451.869	70	N III
454.3	50	W ?
454.748	50	O V (2x227.374)

TABLE II continued

λ	INT	IDENTIFICATION
459.521	50	C III
459.633	50	C III
461.8	50	W ?
462.202	50	O IV (2x227.374)
463.646	40	O V (2x231.823)
467.122	100	O IV (2x233.561)
476.722	70	O IV (2x238.361)
477.146	70	O IV (2x238.573)
478.060	60	Al VII (2x239.030)
480.219	70	Al IV (3x160.073)
481.540	70	Al VII (2x240.770)
483.618	30	C III
485.058	50	Al IV (3x161.686)
486.950	30	Al III
487.520	70	Al VI (2x243.760)
493.587	30	C III
495.126	30	N V (2x247.563)
495.5	50	W
497.0	70	W (2x248.5)
498.9	30	W ?
500.4	50	W (2x250.2)
501.9	50	W ?
502.694	50	Al VIII (2x251.347)
503.8	50	W ?
505.128	30	O IV (2x252.564)
505.4	30	W ?
505.7	30	W ?
506.164	30	O IV (2x253.082)
507.391	70	O III
507.683	70	O III
508.182	70	O III
508.6	30	W ? (2x254.3)
509.4	50	W
510.757	30	N II
511.523	30	C II
516.504	70	O V (3x172.168)
517.069	30	C II
517.937	30	O II
518.242	30	O II
518.805	70	Al V (4x129.729)

TABLE II continued

λ	INT	IDENTIFICATION	
519.246	70	O	VI (3x173.082)
520.2	30	W ?	
520.778	50	O	IV (2x260.389)
521.114	50	O	IV (2x260.556)
521.6	50	W ?	
522.438	50	Al	VII (2x261.219)
523.392	30	Al	V (4x130.848)
525.795	70	O	III
527.536	30	O	III (2x263.768)
530.290	30	C	II
530.9	30	W ?	
533.9	50	W ?	Mo VI ?
536.0	30	W ?	(2x268.0)
537.2	30	W ?	(2x268.9)
537.8	40	W	(2x268.9)
539.8	50	W	(2x269.9)
540.7	40	W ?	Mn IV ?
541.8	30	W ?	Mn IV ?
542.3	50	W ?	Mn IV ?
544.540	70	O	III (2x272.270)
547.6	30	W ?	
550.732	70	O	III (2x275.270)
553.328	70	O	IV
554.514	100	O	IV
555.262	70	O	IV
557.398	100	Al	V (2x278.699)
559.266	50	O	IV (2x279.633)
559.874	50	O	IV (2x279.937)
562.794	70	O	IV (2x281.397)
564.5	30	W ?	
564.663	30	C	II
565.2	30	W	
566.840	50	N	IV (2x283.420)
568.084	50	Al	IX (2x284.042)
570.934	50	Al	VIII (2x285.467)
571.428	50	O	IV (2x285.714)
571.766	50	O	IV (2x285.838)
572.896	30	O	V (2x286.448)
576.5	30	W ?	Fe IV ?
578.460	50	C	IV (2x289.230)

TABLE II continued

λ	INT	IDENTIFICATION	
581.5	30	W ?	Mn IV ?
588.4	30	W	
591.314	30	O	III (2x295.657)
597.818	30	O	III
599.598	70	O	III
600.342	70	O	II (4x150.088)
600.9	30	W ?	(3x200.3)
608.395	70	O	IV
609.2	70	W	
609.829	70	O	IV
610.746	50	O	III
611.192	70	O	III (2x305.596)
611.406	70	O	III (2x305.603)
611.672	70	O	III (2x305.836)
613.1	50	W	
613.8	30	W ?	
614.496	70	Al	VI (2x307.248)
617.120	70	Al	VI (2x308.560)
618.244	70	Al	VII (2x309.122)
619.192	70	Al	VI (2x309.596)
619.704	70	Al	VI (2x309.852)
621.816	70	Al	VI (2x310.908)
623.382	50	O	V (3x207.794)
624.617	30	O	IV
625.852	70	O	IV
627.6	40	W	
629.732	70	O	V
635.180	30	N	II
639.7	60	W ?	
640.292	60	Al	IV (4x160.073)
641.958	70	O	III (2x320.979)
644.148	30	O	II
645.167	50	N	II
646.744	70	Al	IV (4x161.686)
648.054	30	O	V (3x216.018)
648.645	50	Al	IV (5x129.729)
650.900	30	W	(2x325.4)
654.240	40	Al	V (5x130.848)
655.2	30	W ?	Mn IV ?
656.400	50	Al	VIII (2x328.200)

TABLE II continued

λ	INT	IDENTIFICATION	
657.0	30	W ?	Mn IV ?
657.484	30	O	III (2x328.742)
658.3	30	W ?	
658.758	30	O	III
661.056	100	O	IV (3x220.352)
667.6	30	W ?	(2x333.8)
668.6	30	W	
671.391	50	N	II
672.0	40	W ?	(2x336.0)
677.4	70	W ?	(2x338.7)
686.580	30	Al	VII (2x343.290)
687.300	50	Al	VII (2x343.650)
688.672	50	O	V (4x172.168)
690.618	30	O	III (2x345.309)
691.740	60	O	V (3x172.935)
692.328	60	O	V (3x173.082)
693.303	30	O	IV (3x231.101)
700.683	50	O	IV (3x233.561)
702.322	60	O	III
702.899	60	O	III
703.850	60	O	III
704.320	60	Al	VII (2x352.160)
706.000	70	C	III (2x353.9)
707.8	50	W	(2x353.9)
708.4	30	W ?	Mg V ? (2x354.2)
710.666	40	O	II (2x355.333)
713.800	70	W	(2x356.9)
715.719	70	O	IV (3x238.361)
716.800	50	W	
718.484	50	O	II
718.562	50	O	II
722.310	50	Al	VII (3x240.770)
731.280	70	Al	VI (3x243.760)
742.689	30	N	V (3x248.5)
745.5	30	W	(3x248.5)
748.1	50	W ?	Ni III ? O I ?
750.6	50	W	(3x250.2)
754.041	30	Al	VIII (3x251.347)
758.677	70	O	V
759.440	70	O	V

TABLE II continued

λ	INT	IDENTIFICATION	
760.229	70	O	V
761.130	70	O	V
762.001	70	O	V
763.340	30	N	IV
764.357	50	N	IV
765.140	50	N	IV
768.210	70	C	IV (2x384.105)
770.9	30	W	
771.544	30	N	III
774.522	70	O	V
775.957	30	N	II
776.9	10	W ?	Ti IV ? Co III ?
777.657	10	Al	VII (3x259.219)
779.821	70	O	IV
781.167	30	O	IV (3x260.389)
781.668	30	O	IV (3x260.556)
783.657	30	Al	VII (3x261.219)
783.886	30	O	II (2x391.943)
787.710	70	O	IV
788.3	50	W ?	Co III ?
790.103	100	O	IV
790.203	100	O	IV
796.661	10	O	II
797.6	10	W ?	
800.363	50	Al	IV (5x160.073)
802.224	30	O	IV
806.384	30	C	II
806.7	30	W	(3x268.9)
809.3	30	W	
816.0	30	W ?	Fe III ?
816.810	30	O	III (3x272.270)
826.098	40	O	III (3x275.366)
832.754	70	O	II
833.326	70	O	II
833.742	70	O	III
834.462	70	O	II
835.292	70	O	III
838.899	30	O	IV (3x279.633)
839.240	30	C	IV (2x419.620)
839.811	30	O	IV (3x279.937)

TABLE II continued

λ	INT	IDENTIFICATION	
843.2	70	W	(2x421.6)
881.0	10	W	(2x440.5)
903.609	30	C	II
919.364	30	C	III (2x459.521)
921.364	10	O	III
921.982	50	N	IV
923.6	50	W	
925.680	40	Al	VI (3x308.560)
927.036	30	Al	VII (3x309.012)
927.366	30	Al	VII (3x309.122)
928.788	70	Al	VI (3x309.596)
929.556	40	Al	VI (3x309.852)
932.724	50	Al	VI (3x310.908)
936.8	50	W ?	
937.365	30	C	IV (3x312.455)
963.080	50	Al	VII (4x240.770)
969.8	30	W ?	Fe II ? Co III ?
977.027	100	C	III
1014.782	40	O	III (2x507.391)
1015.366	50	O	III (2x507.683)
1016.364	50	O	III (2x508.182)
1031.912	100	O	VI
1036.330	70	C	II
1037.020	70	C	II
1051.590	50	O	III (2x525.795)
1106.656	70	O	IV (2x553.328)
1108.148	70	O	IV (2x554.074)
1109.028	70	O	IV (2x554.514)
1110.524	70	O	IV (2x555.262)
1168.2	50	W	
1175.742	100	C	III
1199.196	50	O	III (2x599.598)
1216.790	50	O	IV (2x608.395)
1219.658	50	O	IV (2x609.829)
1238.800	40	N	V
1242.778	10	N	V
1247.383	10	C	III
1334.520	50	C	II
1335.692	50	C	II
1343.507	30	O	IV

TABLE II concluded

λ	INT	IDENTIFICATION	
1371.287	70	O	V
1468.2	30	W	
1517.350	10	O	V (2x758.677)
1520.460	30	O	V (2x760.229)
1522.260	10	O	V (2x761.130)
1524.000	10	O	V (2x762.001)
1548.195	70	C	IV
1550.768	70	C	IV
1605.750	50	Al	III
1611.850	70	Al	III
1670.786	30	Al	II
1724.575	30	W	
1854.720	70	Al	II
1862.318	70	Al	II
1889.196	10	Al	II

* All intensities are visual estimates of film blackening.

Observations were made to investigate the effect of the variation of the magnetic field on the Argon plasma. The magnetic field was varied from 900 gauss to 2000 gauss. There was no apparent change in relative intensities. The only effect detectable on inspection of the line intensities was that the plasma beam varied with the magnetic field, as indicated by the length of the image spectral lines. These results were obvious upon looking at the film strips, but the contact prints made from these negatives do not show sufficient detail to be included in this report . There was no evidence of any great changes in the relative amounts of ionization with the variations in the magnetic field.

All of the lines listed in Table III as coming from Carbon, Oxygen, and Nitrogen are the result of accidental impurities. These occur in the residual gas, and they may also arise from the plasma beam interacting with the electrodes or the glass walls of the discharge system.

5. Conclusions and Recommendations

The number of unidentified lines in the Tungsten spectrum point out the many gaps found in the literature concerning this spectra. In future work it is suggested that the plasma system be used to produce Tungsten spectra. Tungsten can be evaporated into the plasma system by lowering Tungsten wires into the plasma beam. It was apparent that the electron energy available for excitation has a definite upper limit determined by the anode voltage. At an operating voltage of 140 volts, no spectra requiring an electron energy of 114 ev was observed. Since the

TABLE III

IDENTIFIED LINES OF THE ARGON PLASMA TAKEN AT MIDPOINT OF BEAM

λ	IDENTIFICATION	INT	λ	IDENTIFICATION	INT
303.786	He II	70	488.452	A III	30
327.112	C III	30	488.793	A II	50
328.448	O III	30	489.195	A II	50
345.309	O III	30	490.680	A III	70
346.372	O IV	30	491.121	A III	70
346.688	O IV	30	492.228	A III	30
352.058	N IV	50	492.408	A II	30
353.000	C III	30	492.650	O III	50
371.694	C III	50	501.190	A II	10
395.920	A III	30	502.163	A II	10
396.380	A III	70	503.650	A II	10
396.869	A IV	70	507.537	O III	70
398.546	A IV	50	508.441	A III	100
398.860	A III	10	508.611	A III	100
399.634	A IV	10	510.556	A II	30
429.557	O II	10	511.505	A III	70
436.510	O II	10	512.770	A III	50
443.296	O IV	100	519.327	A II	70
450.734	C III	50	522.792	A II	70
451.869	N III	70	524.680	A II	70
452.226	N III	70	526.497	A II	10
459.462	C III	70	528.650	A II	50
459.633	C III	70	529.900	A III	70
466.530	A III	10	530.495	A II	50
467.390	A III	70	532.413	A III	50
468.467	A III	50	535.580	A III	100
468.956	A III	50	536.745	A III	70
469.831	A III	100	537.459	A III	30
473.025	A III	30	538.312	C III	70
473.918	A III	50	538.788	A III	50
476.432	A III	100	542.912	A II	30
477.625	C III	30	543.203	A II	70
481.848	A III	50	543.731	A II	70
482.548	A III	50	546.177	A II	50
484.116	A III	50	547.165	A II	30
484.445	A III	50	547.460	A II	70
485.150	A III	50	548.781	A II	30
485.515	A III	70	553.470	A III	70
487.025	A III	100	556.817	A II	100
487.988	A III	30	558.321	A III	30

TABLE III continued

λ	IDENTIFI-CATION	INT	λ	IDENTIFI-CATION	INT
560.223	A II	70	704.523	A II	70
572.014	A II	50	718.090	A II	50
573.362	A II	100	723.361	A II	100
576.736	A II	70	725.548	A II	70
577.153	A III	10	730.929	A II	50
578.107	A II	50	740.269	A II	100
578.386	A III	30	744.925	A II	100
578.605	A II	50	748.197	A II	30
579.212	A III	50	754.824	A II	50
580.263	A II	100	762.199	A II	10
583.437	A II	70	769.152	A III	70
597.700	A II	50	792.760	A III (2x396.380)	50
602.858	A II	30	793.778	A IV (2x396.869)	10
604.152	A III	70	797.720	A III (2x398.860)	10
612.372	A II	70	801.086	A IV	10
622.144	C III	10	801.409	A IV	50
623.767	A III	50	834.392	A I	10
625.852	O IV	30	840.029	A IV	30
636.818	A III	50	843.772	A IV	50
637.282	A III	100	850.602	A IV	70
641.364	A III	50	871.099	A III	50
641.808	A III	70	875.534	A III	50
643.256	A III	50	878.728	A III	100
661.869	A II	100	879.622	A III	30
664.562	A II	30	883.179	A III	50
666.011	A II	70	887.404	A III	70
670.945	A II	100	900.362	A IV	30
671.851	A II	100	901.168	A IV	30
676.243	A II	70	919.781	A IV	100
677.952	A II	50	932.052	A IV	70
679.400	A II	100	933.060	A III (2x466.530)	30
683.278	A IV	30	934.780	A III (2x467.390)	70
686.488	A II	10	936.934	A III (2x468.467)	30
690.170	A III	100	937.912	A III (2x468.956)	10
691.037	A II	30	939.662	A III (2x469.831)	50
693.301	A II	30	939.936	A III (2x469.968)	30
695.537	A III	50	946.050	A III (2x473.025)	10
697.489	A II	10	947.836	A III (2x473.918)	50
697.941	A II	10	952.864	A III (2x476.432)	70
698.774	A II	70	963.696	A III (2x481.848)	30

TABLE III concluded

λ	IDENTIFICATION	INT	λ	IDENTIFICATION	INT
965.096	A III (2x482.548)	70	1380.728	A II	10
968.232	A III (2x484.116)	30	1446.722	A II (2x723.361)	10
968.890	A III (2x484.445)	30	1490.643	A II (2x745.321)	10
970.300	A III (2x485.150)	50	1669.304	A III	30
971.030	A III (2x485.515)	30	1669.671	A III	30
974.050	A III (2x487.025)	70	1019.575	A III	10
974.454	A II (2x487.227)	10			
975.976	A III (2x487.988)	10			
977.026	C III	70			
977.585	A II (2x488.792)	30			
978.391	A II (2x489.195)	10			
981.360	A III (2x490.680)	50			
982.242	A III (2x491.121)	30			
1016.882	A III (2x508.441)	70			
1017.222	A III (2x508.611)	10			
1023.010	A III (2x511.505)	50			
1025.540	A III (2x512.770)	10			
1038.654	A II (2x519.327)	30			
1045.594	A II (2x522.792)	30			
1048.218	A I	30			
1049.361	A II (2x524.680)	30			
1059.800	A III (2x529.900)	70			
1066.600	A I	10			
1071.160	A III (2x535.580)	10			
1073.490	A III (2x536.745)	10			
1076.624	C III (2x538.312)	70			
1086.407	A II (2x543.203)	10			
1106.940	A III (2x553.470)	30			
1113.344	A II (2x556.817)	50			
1120.445	A II (2x560.222)	10			
1146.724	A II (2x573.362)	70			
1153.472	A II (2x576.736)	10			
1160.527	A II (2x580.263)	70			
1166.873	A II (2x583.436)	30			
1215.171	He II	100			
1274.564	A III (2x637.282)	50			
1323.738	A II (2x661.869)	30			
1341.890	A II (2x670.945)	10			
1343.703	A II (2x671.857)	30			
1358.800	A II (2x679.400)	10			

ionization potential for W VI is only 61 volts, intermediate stages of ionization of the Tungsten spectra can be investigated.

The use of Aluminum with the Tungsten electrode has obvious disadvantages. The many-line spectrum of Aluminum made identification of the film strip very time consuming. It is suggested that future work with Tungsten electrodes in the vacuum spark be done with an electrode other than Aluminum (the Oxygen spectrum which is usually present offers good calibration points).

Although the curve-fitting computer program in conjunction with the grating equation program are sufficient to calibrate the spectrograph to an accuracy of ± 0.05A, a bootstrap type program or a regenerating type computer program would be desirable for future work.

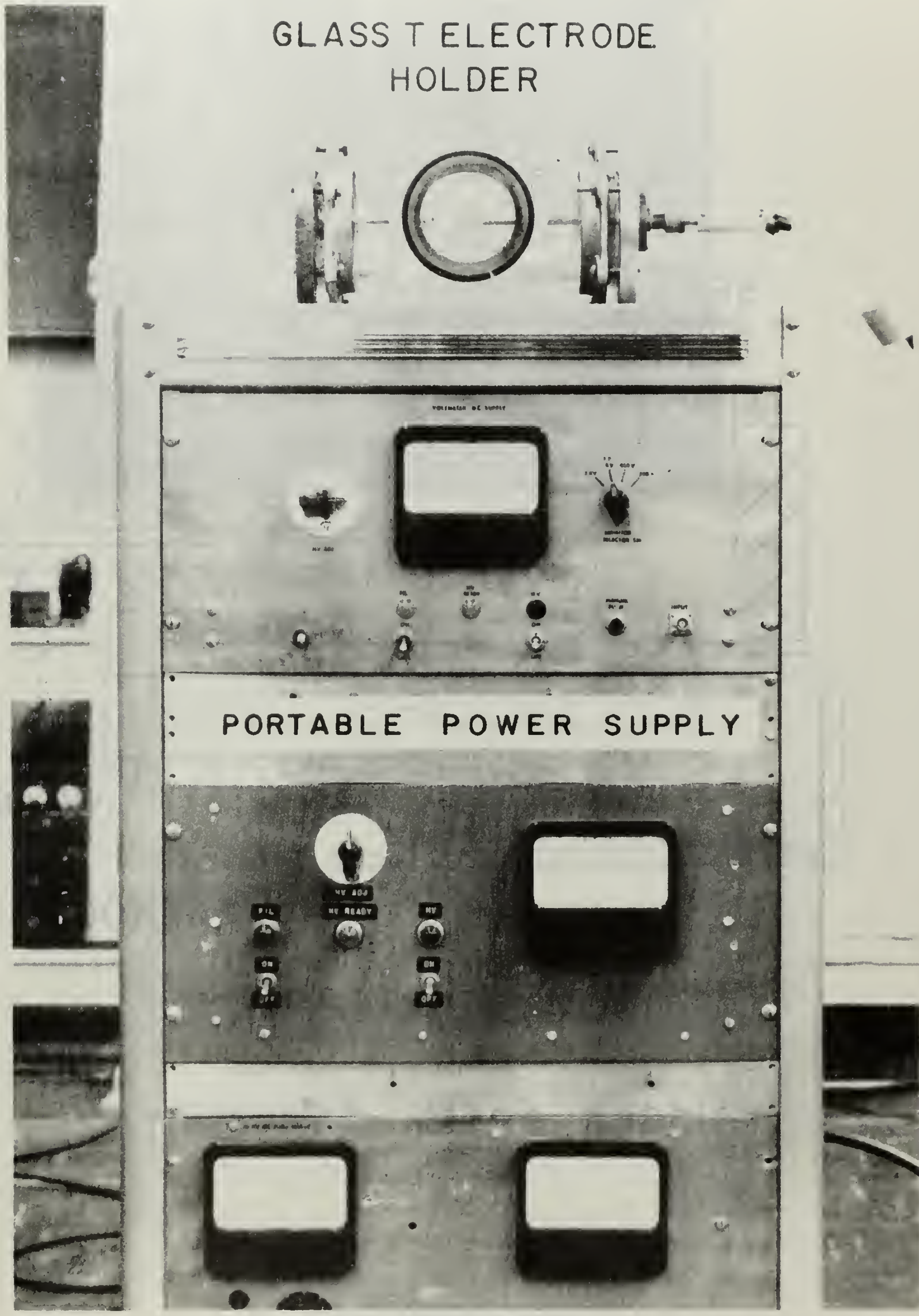

Figure 1. Portable Power Supply with Glass [illegible]lectrode Holder

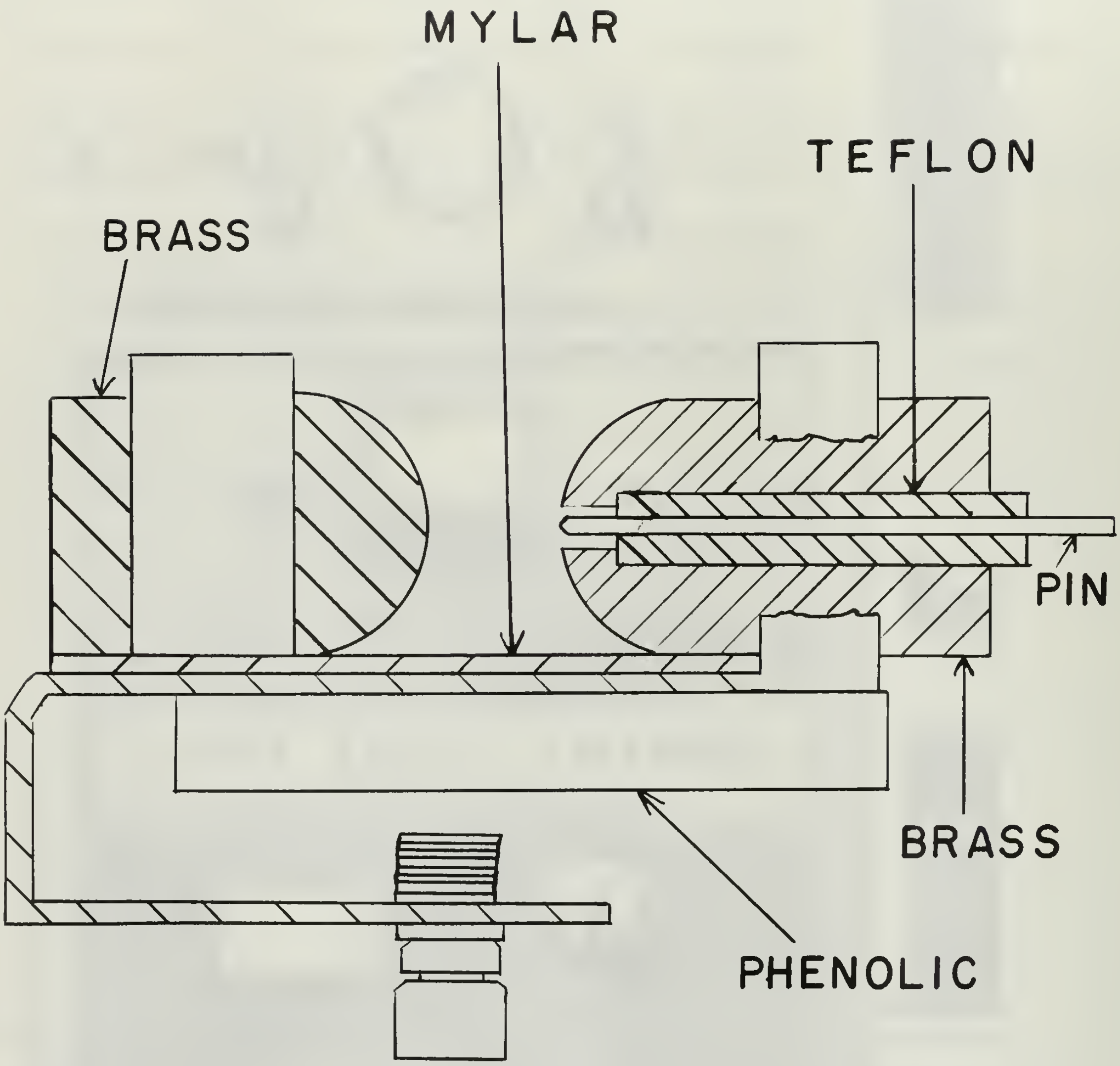

TRIGGER SPARK GAP SWITCH

FIGURE 2

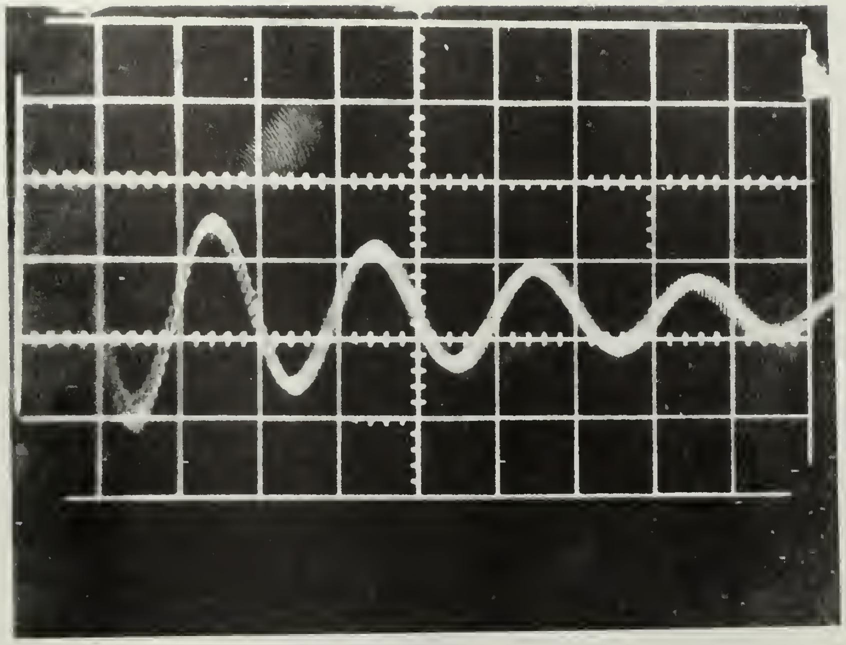

RINGING FREQUENCY
OF SPARK GAP AT
15 KV

FIGURE 3

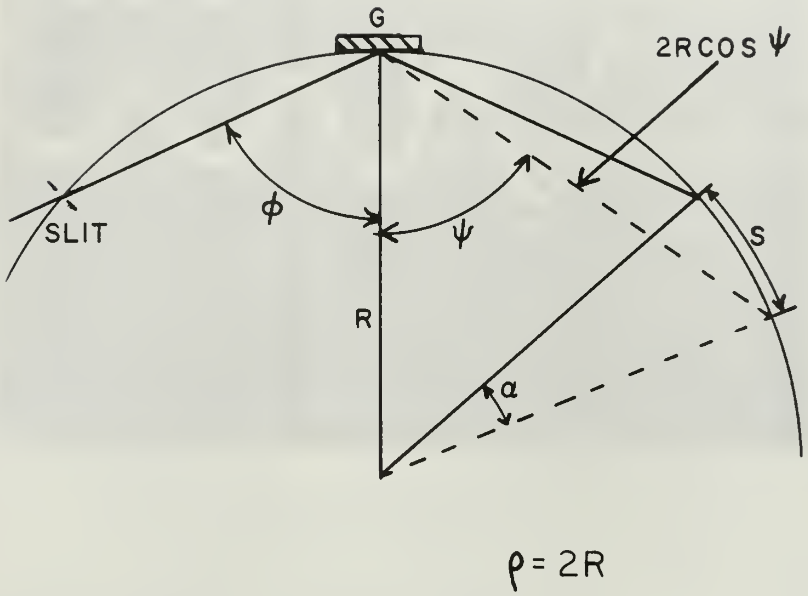

DIAGRAM OF VACUUM GRATING SPECTROGRAPH AT GRAZING INCIDENCE. G, GRATING; S, DISTANCE ON ROWLAND CIRCLE FROM CENTRAL IMAGE; $\alpha = 2(\phi - \psi)$; ρ, RADIUS OF CURVATURE OF THE GRATING.

FIGURE 4

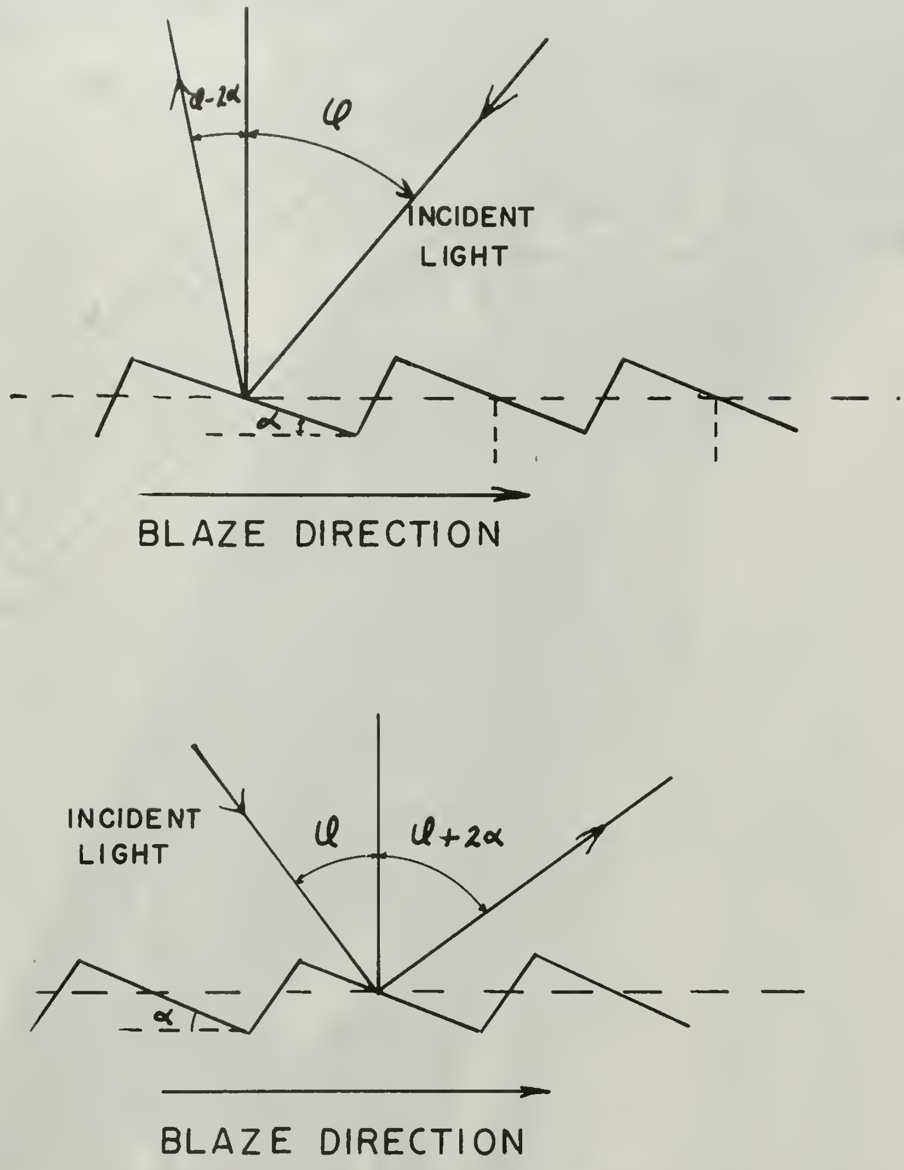

BLAZE ANGLE CONFIGURATIONS SHOWING CHANGE IN BLAZE WAVELENGTH FROM $\varphi-2\alpha$ TO $\varphi+2\alpha$

FIGURE 5

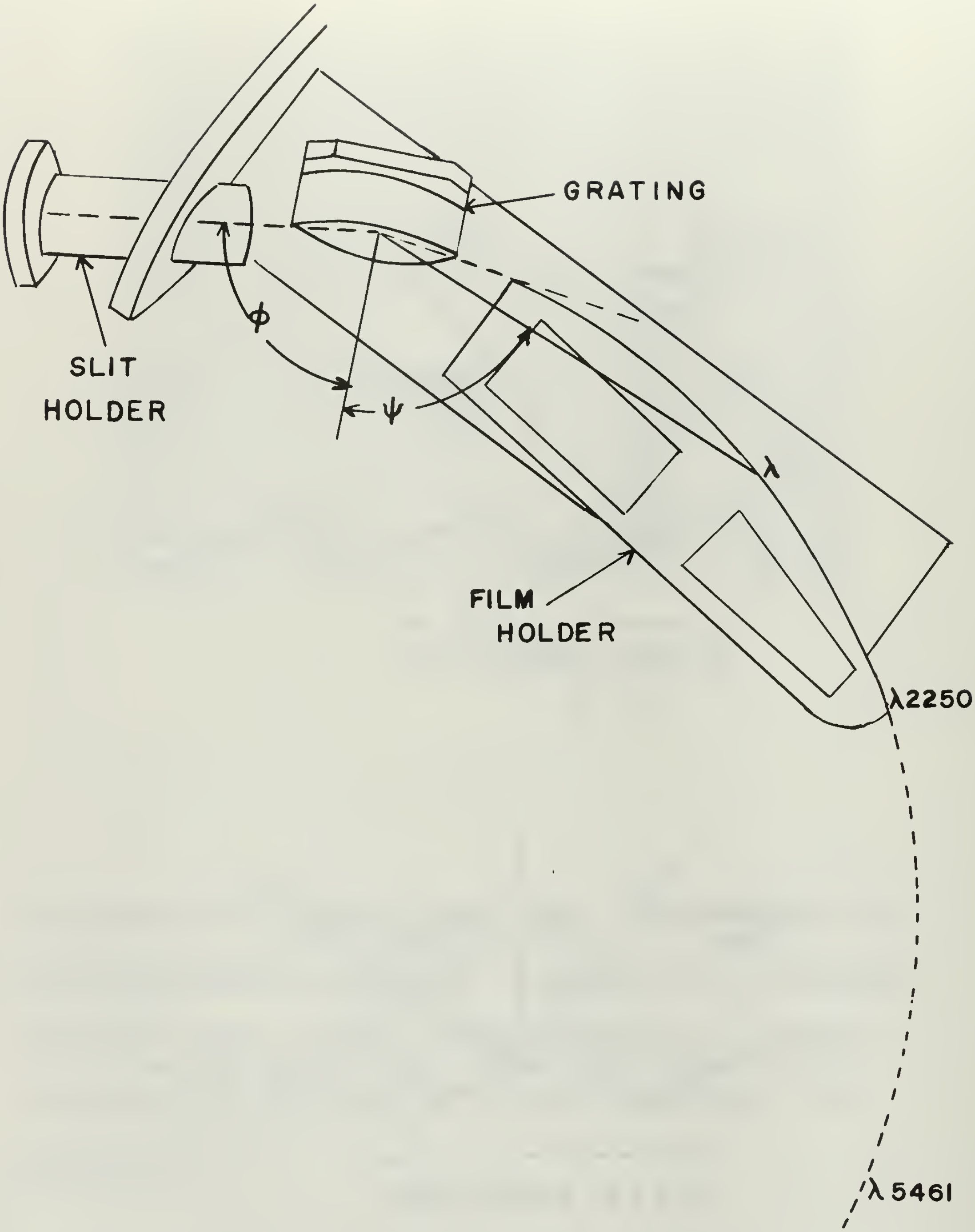

DIAGRAM OF GRAZING INCIDENCE
SPECTROGRAPH

FIGURE 6

TOP VIEW OF SPECTROGRAPH

FIGURE 7

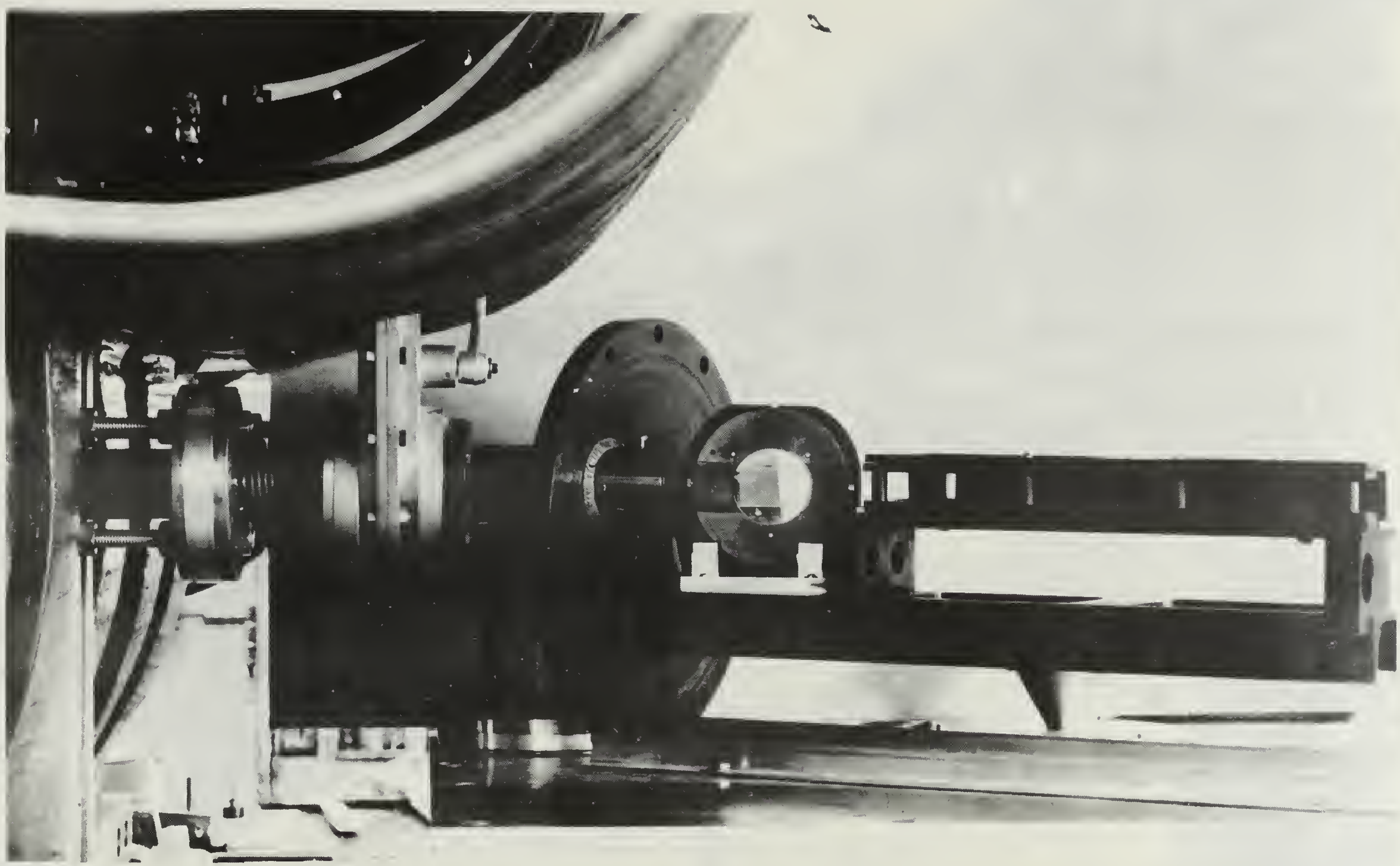

FIG. 8 SIDE VIEW OF GRAZING INCIDENCE SPECTROGRAPH SHOWING CONNECTION TO PLASMA SYSTEM

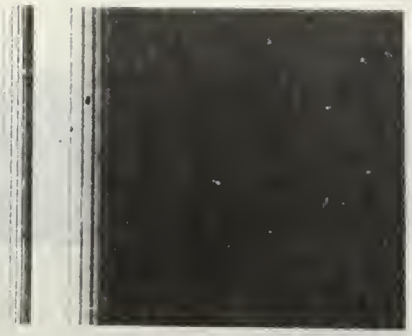

OXYGEN
ABSORPTION
BANDS

ABSORPTION SPECTRUM
OF AIR

FIGURE 9

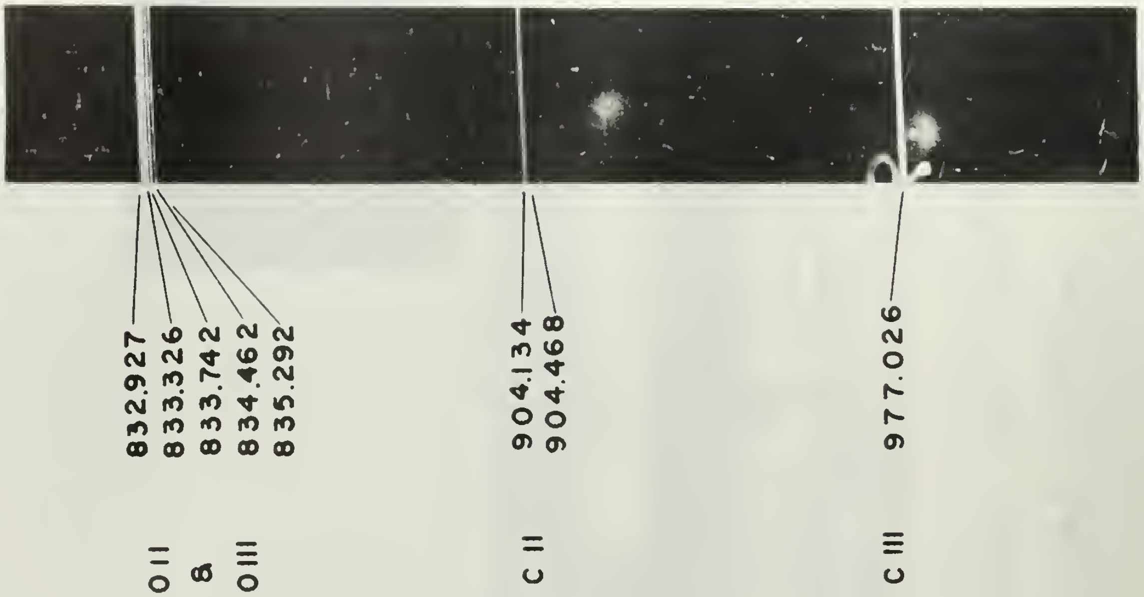

TYPICAL RESULTS
OF
SPARK GAP SPECTRUM

FIGURE 10

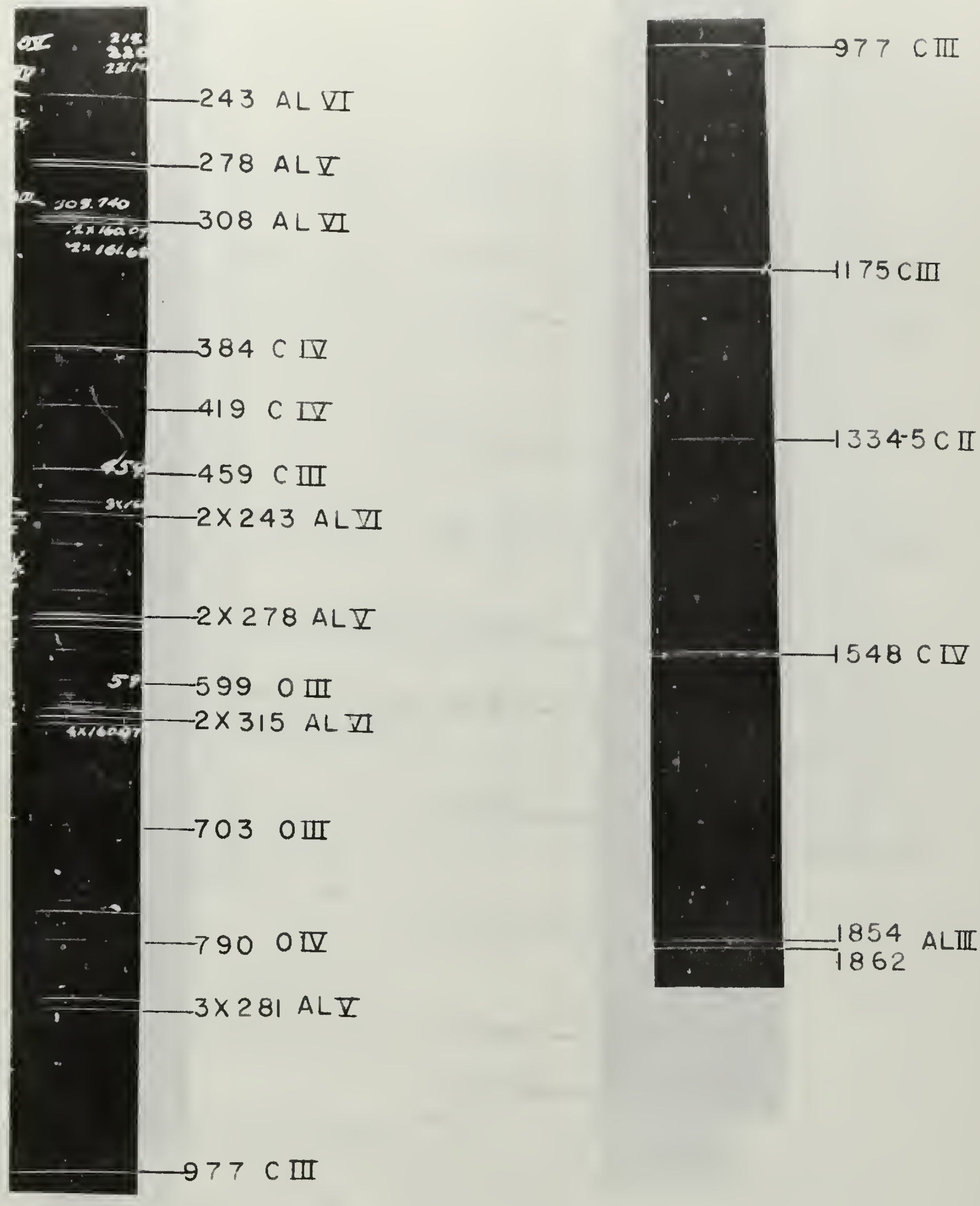

CARBON AND ALUMINUM ELECTRODES

FIGURE 11

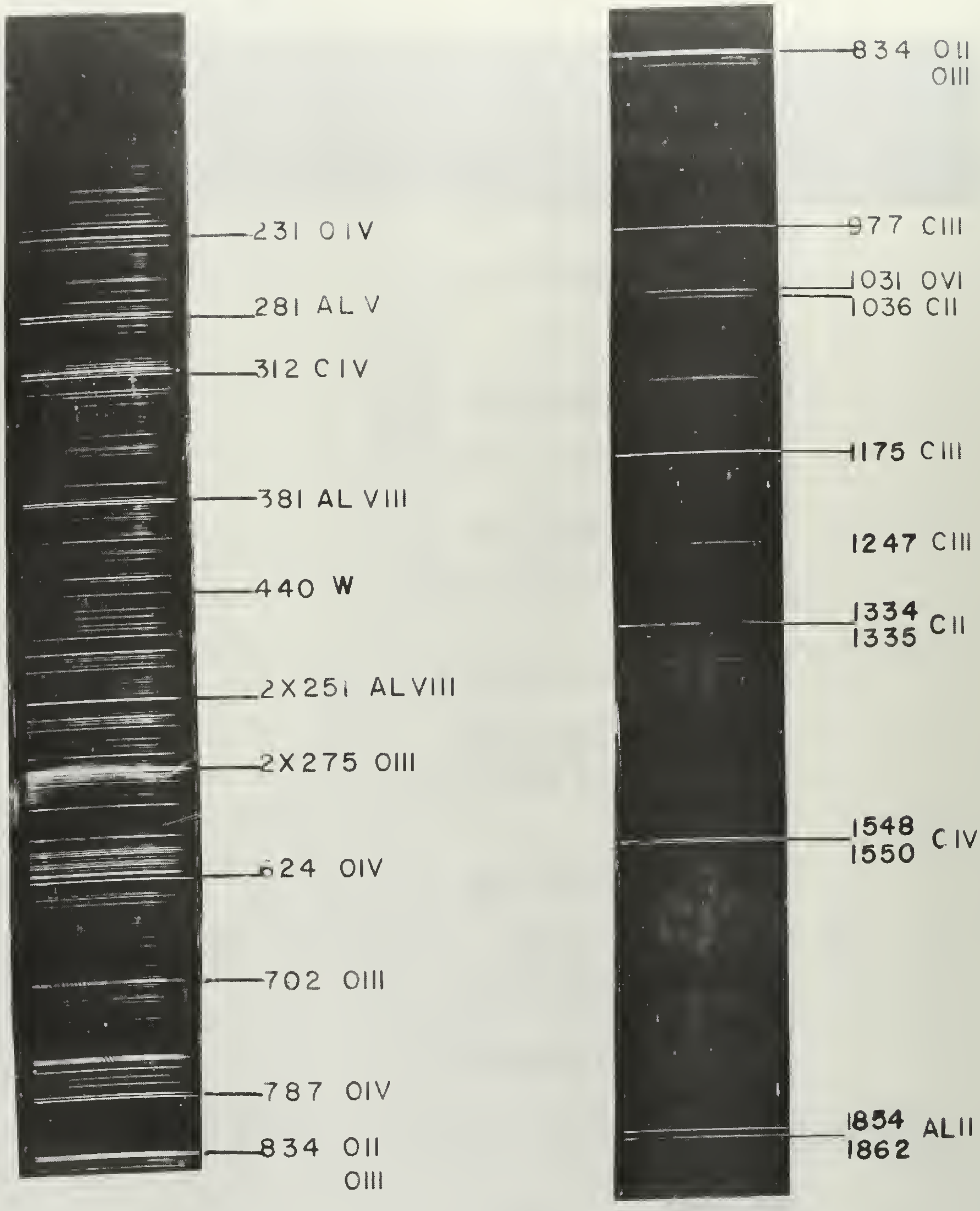

TUNGSTEN AND ALUMINUM ELECTRODES

FIGURE 12

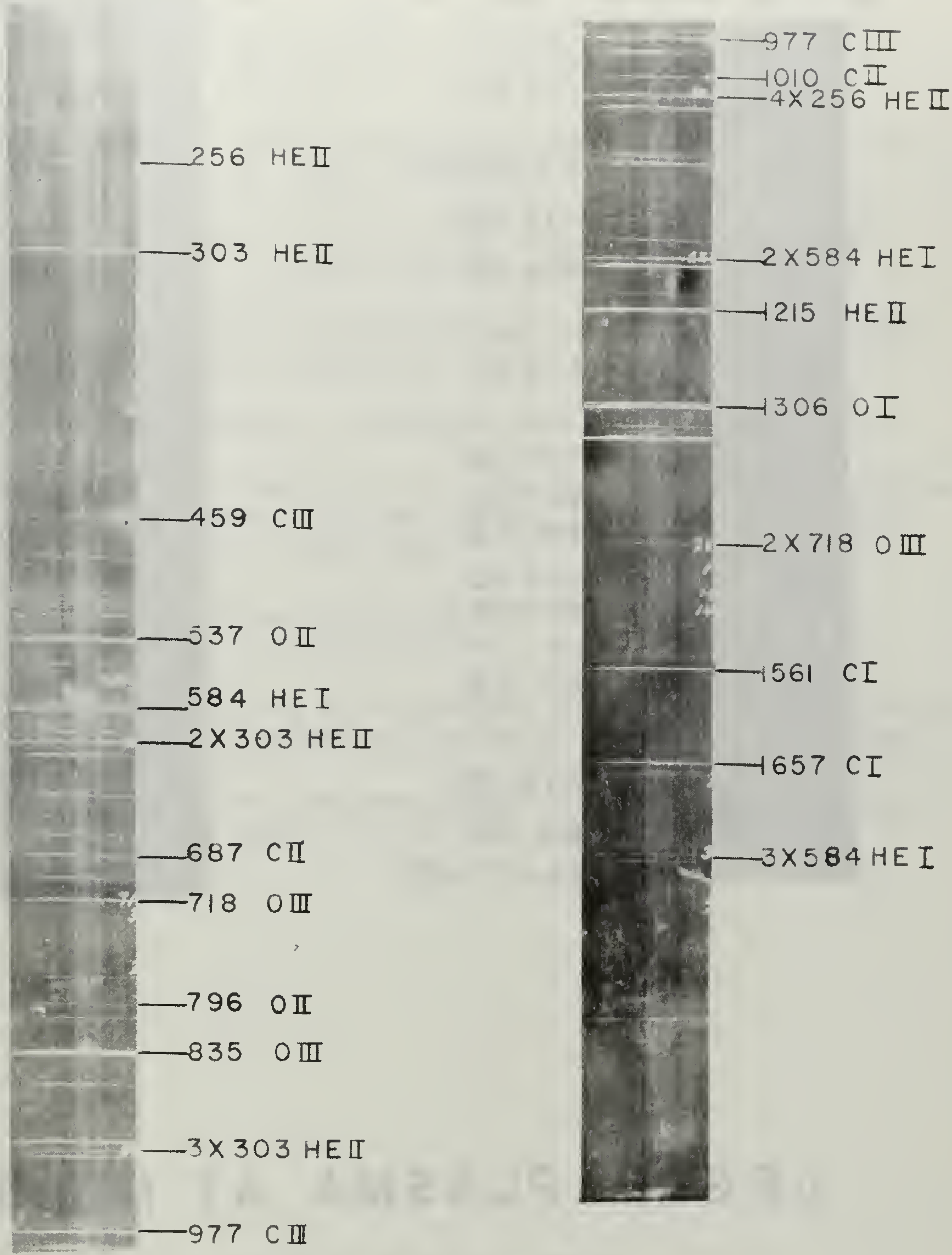

HELIUM PLASMA

FIGURE 13

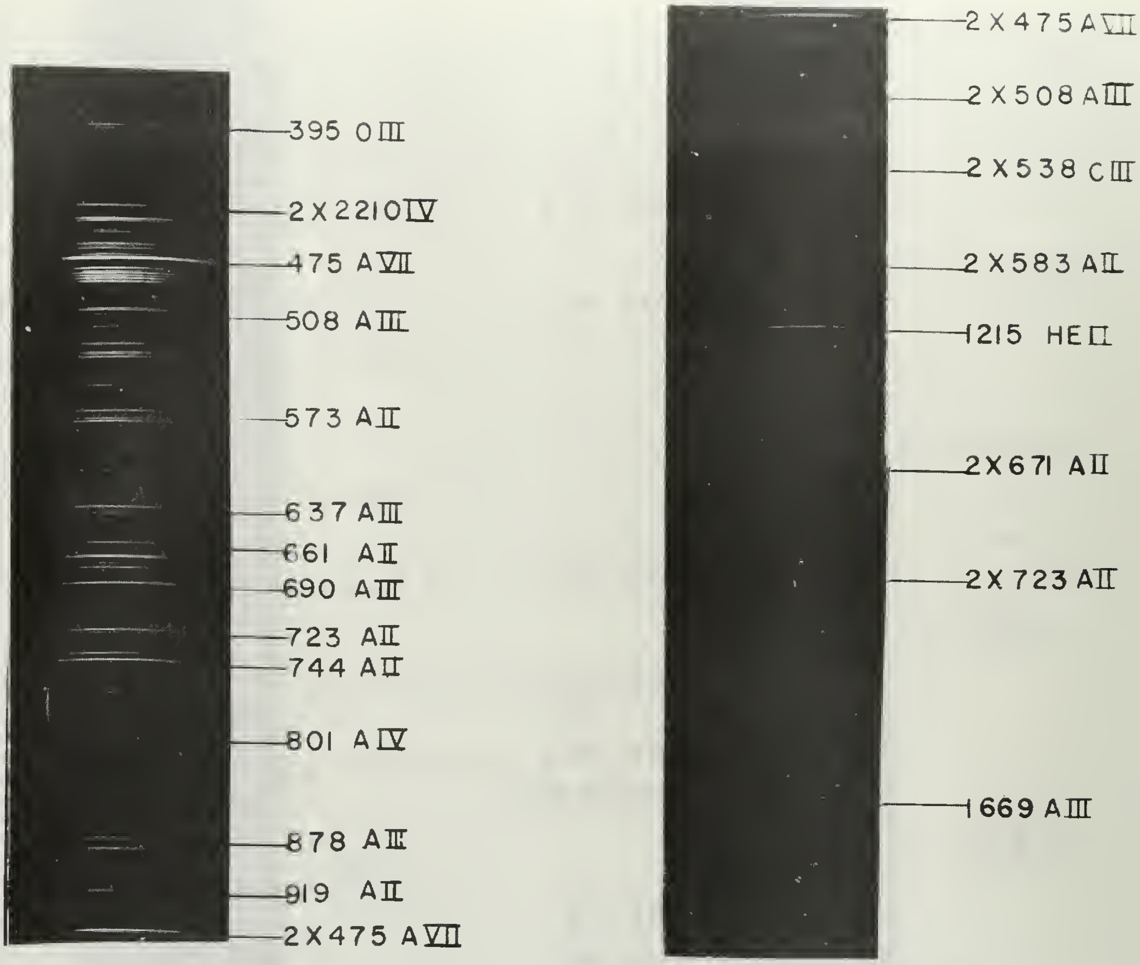

ARGON PLASMA AT MIDPOINT
OF SYSTEM

FIGURE 14

BIBLIOGRAPHY

1. Lupton, W. H., Fast Triggered Spark Switches for a Two Megajoule Capacitor Bank. Proceedings of the Fifth International Conference on Ionization Phenomena in Gases. v. 1, 1961.

2. Beutler, H. G., The Theory of the Concave Grating. J. Opt. Soc. Am., v. 35, May, 1945:311.

3. Mack, J. E., Stehn, J. R., Edlen, B., Concave Grating Spectrograph. J. Opt. Soc. Am., v. 22, 1932:245.

4. Namieko, T., Theory of the Concave Grating. J. Opt. Soc. Am., v. 49, May, 1959:446.

5. Wood, R. W., Optics. The Macmillian Company, 1934.

6. Jacobus, G. F., Madden, R. P., Canfield, L. R., Reflecting Films of Platinum for the Vacuum Ultraviolet. J. Opt. Soc. Am., v. 53, 1963:1084.

7. Tousey, R., Optical Materials for the Far and Extreme Ultraviolet. J. Opt. Soc. Am., v. 53, 1963:524.

8. Kelly, R. L., Vacuum Ultraviolet Emission Lines. University of California Radiation Laboratory Report., 5612, 1959.

9. Raney, J. L., Least Squares Curve Fitting with Orthogonal Polynomials. CO-OP ID, E2 UTEX LSCFWOP, 1962.

APPENDIX I

GRATING EQUATION COMPUTER PROGRAM

```
C   THIS PROGRAM IS IN THE FORM OF THE GRATING EQUATION
C   WITH PH BEING THE ANGLE OF INCIDENCEIN RADIANS,EL
C   THE DISTANCE FROM AN ARBITARY REFERENCE LINE, AS IS
C   THE ANGLE OF REFRACTION, ELR IS THE DIFFERENCE OF THE
C   ANGLES OF REFRACTION AND THE ANGLE OF INCIDENCE AND
C   DSDLAM IS THE DISPERSION

      PROGRAM VUVGISER
      PH = 1.4224431
      SP = SINF(PH)
      X = 0.0
      DX = 0.50
      DO 10 I=1,130
      WAVEL = 1548.195 - X
      ALFA = (SP - WAVEL/16666.67)
      AS = ASINF(ALFA)
      ELR = AS - PH
      EL = ELR*998.0/(16666.67*COSF(AS))
      PRINT 100,EL,WAVEL,ALFA,AS,ELR,DSDLAM
  100 FORMAT(6F20.6)
   10 X = X + DX
      STOP
      END
      END
```

APPENDIX II

Least Square Curve Fitting with Orthognal Polynomials

This computer program utilizes least squares curve fitting using orthogonal polynomials, and computes the polyndmial of degree K,(K=100), that best fits the data points. Upon completion of the fitting process, the program can evaluate the polynomial at the various abscissa points to obtain new ordinates. These ordinates may then be compared with the orginal ordinates to test the accuracy of the fit.

The easily identified lines of a spectrum are classified as to position and wavelength, and become the original abscissa and ordinate points for the program. The unknown lines are classified as to position only and form the data points for the fitting polynomial. The print-out includes the original abscissa and ordinates points, and the computed ordinate points. The unknown lines now have a computed wavelength corresponding to their position, and have an accuracy determined by the error between the original and computed ordinates points at positions close by.

The orginal abscissa and ordinate points are gradually increased as more and more lines become identified. Broad lines are omitted to improve the accuracy, and the computer print-out is continuely checked to determine the degree of polynomial that gives the best fit.

By limiting the region of coverage to about 400A, errors can easily be determined and corrected. For example, the Tungsten spectrum was satisfactorily identified after 7 separate runs.

INITIAL DISTRIBUTION LIST

		No. Copies
1.	Defense Documentation Center Cameron Station Alexandria, Virginia 22314	20
2.	Library Naval Postgraduate School Monterey, California 93940	2
3.	Professor Raymond L. Kelly Department of Physics Naval Postgraduate School Monterey, California 93940	5
4.	Lcdr L. E. Kaufman, USN VA-125 N.A.S. Lemoore Lemoore, California 93246	2
5.	Commander, Naval Ordnance Systems Command Hqs., Washington, D. C. 20360	1
6.	Commander, Naval Air Systems Command Hqs. Washington, D. C. 20360	1

UNCLASSIFIED
Security Classification

DOCUMENT CONTROL DATA - R&D

(Security classification of title, body of abstract and indexing annotation must be entered when the overall report is classified)

1. ORIGINATING ACTIVITY *(Corporate author)*
Ordnance Engineering Programs
Naval Postgraduate School

2a. REPORT SECURITY CLASSIFICATION
UNCLASSIFIED

2b. GROUP

3. REPORT TITLE
Investigations in the Vacuum Ultraviolet using a Grazing Incidence Spectrograph

4. DESCRIPTIVE NOTES *(Type of report and inclusive dates)*
Thesis

5. AUTHOR(S) *(Last name, first name, initial)*
Kaufman, Larry E.

6. REPORT DATE	7a. TOTAL NO. OF PAGES	7b. NO. OF REFS
	58	9

8a. CONTRACT OR GRANT NO.

b. PROJECT NO. N/A

c.

d.

9a. ORIGINATOR'S REPORT NUMBER(S)

9b. OTHER REPORT NO(S) *(Any other numbers that may be assigned this report)*

10. AVAILABILITY/LIMITATION NOTICES
[redacted]
This document has been approved
release and sale; its distribution [illegible] GDL 9/1/69

11. SUPPLEMENTARY NOTES

12. SPONSORING MILITARY ACTIVITY

13. ABSTRACT

A grazing incidence vacuum spectrograph has been used for studies on high temperature plasmas and to investigate the Tungsten spectra produced by a vacuum spark source. The spectrograph uses a concave grating which has a 1-meter radius of curvature and 600 grooves per mm. Incident light strikes the grating at an angle of 81.5°, and the diffracted light is collected on a film strip (15-inches long, 35 mm SWR film) which is held along the Rowland Circle.

Design and details of construction of the spectrograph and the vacuum spark source are presented. A total of 47 new Tungsten lines were identified from the vacuum spark source using Aluminum and Tungsten electrodes.

DD FORM 1 JAN 64 1473

UNCLASSIFIED
Security Classification

14 KEY WORDS	LINK A		LINK B		LINK C	
	ROLE	WT	ROLE	WT	ROLE	WT
Grazing Incidence Spectrograph						
Blaze Angle						
Tungsten Spectra						

DD FORM 1 NOV 65 1473 (BACK)

S/N 0101-807-6821